British Journal of Pharmacology

DOI:10.1111/j.1476-5381.2011.01500.x
www.brjpharmacol.org

RESEARCH PAPER

# Decreased production of neuronal NOS-derived hydrogen peroxide contributes to endothelial dysfunction in atherosclerosis

**Correspondence**
Virginia S Lemos, Department of Physiology and Biophysics, ICB, Federal University of Minas Gerais, Av. Antônio Carlos, 6627, Pampulha. 31270-901, Belo Horizonte, MG, Brazil. E-mail: vslemos@icb.ufmg.br

**Keywords**
nNOS; $H_2O_2$; endothelial dysfunction; atherosclerosis

**Received**
20 October 2010
**Revised**
26 February 2011; 27 April 2011
**Accepted**
14 May 2011

LSA Capettini[1], SF Cortes[2], JF Silva[1], JI Alvarez-Leite[3] and VS Lemos[1]

[1]*Department of Physiology and Biophysics, Biological Sciences Institute, Federal University of Minas Gerais, Belo Horizonte, Brazil,* [2]*Department of Pharmacology, Biological Sciences Institute, Federal University of Minas Gerais, Belo Horizonte, Brazil, and* [3]*Department of Biochemistry and Immunology, Biological Sciences Institute, Federal University of Minas Gerais, Belo Horizonte, Brazil*

## BACKGROUND AND PURPOSE

Reduced NO availability has been described as a key mechanism responsible for endothelial dysfunction in atherosclerosis. We previously reported that neuronal NOS (nNOS)-derived $H_2O_2$ is an important endothelium-derived relaxant factor in the mouse aorta. The role of $H_2O_2$ and nNOS in endothelial dysfunction in atherosclerosis remains undetermined. We hypothesized that a decrease in nNOS-derived $H_2O_2$ contributes to the impaired vasodilatation in apolipoprotein E-deficient mice ($ApoE^{-/-}$).

## EXPERIMENTAL APPROACH

Changes in isometric tension were recorded on a myograph; simultaneously, NO and $H_2O_2$ were measured using carbon microsensors. Antisense oligodeoxynucleotides were used to knockdown eNOS and nNOS *in vivo*. Western blot and confocal microscopy were used to analyse the expression and localization of NOS isoforms.

## KEY RESULTS

Aortas from $ApoE^{-/-}$ mice showed impaired vasodilatation paralleled by decreased NO and $H_2O_2$ production. Inhibition of nNOS with L-$Arg^{NO2}$-L-Dbu, knockdown of nNOS and catalase, which decomposes $H_2O_2$ into oxygen and water, decreased ACh-induced relaxation by half, produced a small diminution of NO production and abolished $H_2O_2$ in wild-type animals, but had no effect in $ApoE^{-/-}$ mice. Confocal microscopy showed increased nNOS immunostaining in endothelial cells of $ApoE^{-/-}$ mice. However, ACh stimulation of vessels resulted in less phosphorylation on Ser852 in $ApoE^{-/-}$ mice.

## CONCLUSIONS AND IMPLICATIONS

Our data show that endothelial nNOS-derived $H_2O_2$ production is impaired and contributes to endothelial dysfunction in $ApoE^{-/-}$ aorta. The present study provides a new mechanism for endothelial dysfunction in atherosclerosis and may represent a novel target to elaborate the therapeutic strategy for vascular atherosclerosis.

### Abbreviations

$ApoE^{-/-}$, apolipoprotein E-deficient mice; AS-ODN, antisense oligodeoxynucleotide; EDRF, endothelium-derived relaxing factor; eNOS, endothelial NOS; iNOS, inducible NOS; KD, knockdown; LDL, low density lipoprotein; MM-ODN, mismatch oligodeoxynucleotide; nNOS, neuronal NOS

## Introduction

Atherosclerosis is the major cause of cardiovascular disease, which still has the leading position in morbidity and mortality in the Western world. Endothelial dysfunction is considered an earlier marker for atherosclerosis, preceding angiographic or ultrasonic evidence of atherosclerotic plaques (Busse and Fleming, 1996; Luscher and Barton, 1997; Ross, 1999; Cai and Harrison, 2000; Higashi *et al.*, 2009a).

As the major regulator of vascular homeostasis, the endothelium not only modulates the tone of the underling vascular smooth muscle but also inhibits several pro-atherogenic processes, including smooth muscle cell proliferation and migration, platelet aggregation, oxidation of low-density lipoproteins (LDL), monocyte and platelet adhesion and synthesis of inflammatory cytokines, thus exhibiting important anti-atherogenic effects (Vanhoutte, 1986; Kubes *et al.*, 1991; Freedman *et al.*, 1999; Shimokawa, 1999; Leopold and Loscalzo, 2009; Sima *et al.*, 2009). Many of these effects are largely mediated by NO.

NO is produced by NOS enzymes classified as endothelial NOS (eNOS), neuronal NOS (nNOS) and inducible NOS (iNOS) (Alderton *et al.*, 2001). Although, eNOS is predominantly expressed in endothelial cells, and nNOS in neurons, many tissues express more than one isoform. The vasculature has the potential to express nNOS and eNOS (Rosenblum and Murata, 1996; Boulanger *et al.*, 1998; Toda and Okamura, 2003; Bachetti *et al.*, 2004; Capettini *et al.*, 2008). A physiologically relevant role for nNOS has been attributed in the modulation of myogenic tone (Fleming, 2003), systemic arterial pressure (Kurihara *et al.*, 1998) and cerebral blood flow (Hagioka *et al.*, 2005).

Recently, we have shown that nNOS is constitutively expressed in the endothelium of the mouse aorta and, besides NO, also produces hydrogen peroxide ($H_2O_2$) (Capettini *et al.*, 2008; 2010). $H_2O_2$ has been considered an endothelium-derived hyperpolarizing factor (EDHF) in mesenteric (Matoba *et al.*, 2000; 2002), coronary (Miura *et al.*, 2003; Yada *et al.*, 2003) and cerebral arteries (Sobey *et al.*, 1997; Iida and Katusic, 2000). In the mouse aorta, nNOS-derived $H_2O_2$ equally contributes with eNOS-derived NO to endothelium-dependent vascular relaxation (Capettini *et al.*, 2010).

nNOS has been recently proposed as a new anti-atherogenic factor (Tsutsui, 2004; Kuhlencordt *et al.*, 2006; Schodel *et al.*, 2009) preventing neointima formation in carotid artery ligation model (Morishita *et al.*, 2002). An increase in nNOS expression was found in conductance vessels with atherosclerotic plaque in human and murine models (Wilcox *et al.*, 1997). In addition, gene deletion of nNOS in apolipoprotein E-deficient mice ($ApoE^{-/-}$) accelerates atherosclerotic plaque formation in the aortic root and descending thoracic aorta (Kuhlencordt *et al.*, 2006; Schodel *et al.*, 2009).

Murine models of atherosclerosis have impaired endothelium-dependent relaxation (Busse and Fleming, 1996; Bouloumie *et al.*, 1997; Luscher and Barton, 1997; Deckert *et al.*, 1999; Rabelo *et al.*, 2003; Sima *et al.*, 2009). Chemical inactivation and reduced biosynthesis of NO have been described as key mechanisms responsible for endothelial dysfunction in aortas from atherosclerotic animals (Bouloumie *et al.*, 1997; Laursen *et al.*, 2001; Higashi *et al.*, 2009b). The role of $H_2O_2$ and nNOS to endothelial dysfunction in atherosclerosis remains so far unknown. The aim of this study was to investigate the contribution of nNOS-derived $H_2O_2$ to the impaired endothelium-dependent relaxation in a murine model of atherosclerosis. We hypothesize that an impairment of the nNOS/$H_2O_2$ axis might contribute to endothelium dysfunction in $ApoE^{-/-}$ mice.

## Methods

### *Animals*

All animal care and experimental procedures complied with guidelines for the humane use of laboratory animals and were approved by the animal ethics committee of the Federal University of Minas Gerais (protocol # 155/10). We used 12 week-old male homozygous $ApoE^{-/-}$ (29.7 ± 0.4 g; $n$ = 22) mice and age-matched wild-type C57BL/6J (28.0 ± 2.6 g; $n$ = 25) mice. $ApoE^{-/-}$ mice were originally obtained from Jackson Laboratories (Bar Harbor, ME, USA) and breed in animal facilities of Federal University of Minas Gerais. C57BL/6J mice were obtained from CEBIO/ICB (UFMG, Brazil). All animals were fed a non-atherogenic diet. For metabolic characterization of the animals and morphological and histological characterization of the aorta, see online supporting information and Figure S1.

### *Simultaneous measurements of NO, $H_2O_2$ and vascular function*

Simultaneous measurements of vasodilatation, NO and $H_2O_2$ production, induced by ACh were performed as previously described (Capettini *et al.*, 2010). In brief, rings from the thoracic aorta were obtained, mounted in organ bath system, washed in Krebs–Henseleit solution (in mmol·$L^{-1}$: 110.8 NaCl, 5.9 KCl, 25.0 $NaHCO_3$, 1.07 $MgSO_4$, 2.49 $CaCl_2$, 2.33 $NaH_2PO_4$ and 11.51 glucose, pH 7.4) and stabilized for 60 min. Concentration–response curves to ACh were constructed in vessels precontracted to the same tension level (approximately 2.5 mN.mm) with submaximal concentrations of phenylephrine (0.03–0.1 μmol·$L^{-1}$). Measurements of isometric tension were recorded by a force transducer (World Precision Instruments, Inc., Sarasota, FL, USA) and were fed to an amplifier-recorder (TBM-4 model; World Precision Instruments, Inc.) and to a personal computer equipped with an analogue-to-digital converter board (AD16JR; World Precision Instruments Inc.). Changes in isometric tension were analysed using WinDaq Data Acquisition software (Dataq® Instruments, Akron, OH, USA). Carbon microsensors with a NO and $H_2O_2$ permeable membrane (ISO-NOPF100 and ISO-HPO100, respectively; World Precision Instruments Inc.) were placed next to the lumen of vessels before ACh (0.001–300 μmol·$L^{-1}$) stimulus and currents (nA) were measured. NO and $H_2O_2$ concentrations were determined by calibrations curves of known concentrations of S-nitroso-n-acetylpeniciline (SNAP, 0.2 to 500 nmol·$L^{-1}$; World Precision Instruments, Inc.) or $H_2O_2$ (0.001 to 10 μmol·$L^{-1}$; Merck, Darmstadt, Germany) freshly prepared.

### *Antisense oligonucleotides*

Antisense oligodeoxynucleotides (AS-ODN) were used to knockdown *in vivo* eNOS (eNOS-KD) and nNOS (nNOS-KD) in wild-type and $ApoE^{-/-}$ mice (Capettini *et al.*, 2008; 2010). The 19-base phosphorothioated AS-ODN were constructed

based on the mouse sequence. We used the following specific sequences: 5′-CTCTTCAAGTTGCCCATGT-3′ for eNOS and 5′-AACGTGTGCTCTTCCATGG-3′ for nNOS (GenBank accession numbers NM 008713 and NM 008712) purchased from Eurogentech North America Inc. (San Diego, CA, USA). The phosphorothioated mismatch ODN (MM-ODN) sequence with the base composition, 5′-GTCTTGAACTTCCCGATCT-3′, was used as control ODN.

### In vivo *treatment with AS-ODN to nNOS and eNOS*

The mice received 2 nmol AS-ODN or MM-ODN i.v., 24 and 48 h before the experiments (Capettini *et al.*, 2008; 2010). The AS-ODN and MM-ODN were dissolved in a total volume of 200 µL saline and injected with a 26-gauge needle in the penile vein. The efficiency of the AS-ODN to block expression of nNOS and eNOS was evaluated by Western blot analysis and by functional assay of ACh-induced vasorelaxation.

### *Western blot analysis*

Western blot was performed as previously described with some modifications (Capettini *et al.*, 2008). Aortic rings were dissected and stabilized in Krebs–Henseleit solution for 15 min. ACh (100 µmol·L$^{-1}$) was then applied, and the aortas were collected 8 min after and immediately frozen at –80°C. Non-stimulated aortas were used for basal condition assays. The frozen aortas were homogenized in lyses buffer (in mmol·L$^{-1}$): 150 NaCl, 50 Tris–HCl, 5 EDTA.2Na, and 1 $MgCl_2$ containing 1% Triton X-100 and 0.5% SDS plus a cocktail of protease inhibitors (SigmaFAST®, Sigma, St. Louis, MO, USA) and phosphatase inhibitors (20 mmol·L$^{-1}$ NaF; 0.1 mmol·L$^{-1}$ $Na_3VO_4$); 50 µg of protein were denatured and separated in denaturing SDS/7.5% polyacrylamide gel. Proteins were transferred onto a polyvinylidene fluoride membrane (Immobilon P; Millipore, MA, USA). Blots were blocked at room temperature with 2.5% non-fat dry milk in PBS plus 0.1% Tween 20 before incubation with rabbit polyclonal anti-nNOS (1:1000), mouse monoclonal anti-nNOS Ser852 (1:1000), rabbit polyclonal anti-eNOS (1:1000), goat polyclonal anti-eNOS Ser1177 (1:1000), goat polyclonal anti-eNOS Thr495 (1:1000) or rabbit polyclonal anti-β-actin (1:3000), at room temperature. Immunoreactive bands were detected using the Immobilon Western Chemiluminescent HRP Substrate (Millipore, Billerica, MA, USA). Rabbit polyclonal anti-eNOS was purchased from Sigma. The other antibodies were purchased from Santa Cruz Biotechnology (Santa Cruz, CA, USA).

### *Confocal microscopy*

Thirty percent sucrose (in PBS)-fixed cryosections (6 µm) of the thoracic aorta from wild-type and ApoE$^{-/-}$ mice were rinsed in wash buffer (3% BSA + 0.3% Triton X-100, in PBS). Following appropriate blocking procedures (3% BSA in PBS; 30 min), cross-reactivity of secondary antibodies with the alternating primary antibodies was removed. Slides were incubated with mouse monoclonal anti-GAPDH (1:100; Santa Cruz Biotechnology) and rabbit anti-nNOS (1:50; Santa Cruz Biotechnology) or rabbit anti-eNOS (1:50; Sigma) overnight at 4°C followed by incubation with goat anti-rabbit secondary antibody conjugated with Alexa Fluor 633 (1:500; Invitrogen, Carlsbad, CA, USA) and goat anti-mouse secondary antibody conjugated with Alexa Fluor 488 (1:500; Invitrogen) for 1 h. The sections were examined with a Zeiss LSM 510 confocal microscope (Thornwood, NY, USA) with excitation at 488/633 nm and emission at 505–530/650 nm. The fluorescence (arbitraries unities) intensity was measured using ImageJ® software 1.42q (Wayne Rasband, NIH). Ten fields per slide of endothelial and media layers were measured. The mean of fluorescence from each slide was plotted and analysed using GraphPad Prism 4 (Graphpad Software Inc., La Jolla, CA, USA). Fluorescence intensity in ApoE$^{-/-}$ aorta was expressed as fold increase compared with wild-type animals.

### *Statistical analysis*

Results are expressed as mean ± SEM. Two-way ANOVA with Bonferroni's multiple comparisons post-test was used to compare concentration–response curves. Student's *t*-test was used in the other experiments. All statistical analyses were considered significant when $P < 0.05$.

### *Materials*

ACh, catalase, N$^{\omega}$-nitro-L-arginine methyl ester hydrochloride, L-Arg$^{NO2}$-L-Dbu-$NH_2$ 2TFA and phenylephrine were purchased from Sigma.

## Results

### *Role of nNOS on ACh-induced vasodilatation, and NO and $H_2O_2$ production in the ApoE$^{-/-}$ mice aorta*

Aortic rings from ApoE$^{-/-}$ mice showed a reduced vasodilatation in response to ACh ($E_{max}$ = 54.0 ± 4.1%; $P < 0.001$), compared with wild-type animals ($E_{max}$ = 95.04 ± 1.55%; Figure 1A,B). The impaired vasodilator response in ApoE$^{-/-}$ arteries was accompanied by a severe impairment in NO (Figure 1A) and $H_2O_2$ production (Figure 1B). Non-selective inhibition of NOS with L-NAME (300 µmol·L$^{-1}$) abolished the vasodilator response (Figure 2A) and NO production (Figure 2B) in wild-type and ApoE$^{-/-}$ mice. $H_2O_2$ production was almost completely abolished by L-NAME in wild-type vessels. However, in ApoE$^{-/-}$ animals, the production of $H_2O_2$ was very low and not affected by L-NAME (Figure 2C). Interestingly, selective inhibition of nNOS with 1 µmol·L$^{-1}$ L-Arg$^{NO2}$-L-Dbu, a concentration that inhibits nNOS without affecting eNOS (Huang *et al.*, 1999), reduced ACh-induced relaxation in wild-type but not in ApoE$^{-/-}$ aorta (Figure 2D), suggesting a reduction in nNOS function and or expression in ApoE$^{-/-}$ vessels. In wild-type animals, nNOS inhibition modestly decreased NO (Figure 2E) but abolished $H_2O_2$ production (Figure 2F). In ApoE$^{-/-}$ animals, NO and $H_2O_2$ production were not affected by selective nNOS inhibition. Catalase (2400 U·mL$^{-1}$), which specifically decomposes $H_2O_2$ into oxygen and water, reduced vasodilatation in wild-type animals in the same proportion as that obtained with nNOS inhibition. However, catalase had no effect in ApoE$^{-/-}$ aortas (Figure S2). Vasorelaxation in response to $H_2O_2$ was not different between the strains (Figure S3).

### *Expression and localization of eNOS and nNOS*

Western blot analysis showed that expression of eNOS and nNOS were increased in the aortas from ApoE$^{-/-}$ mice

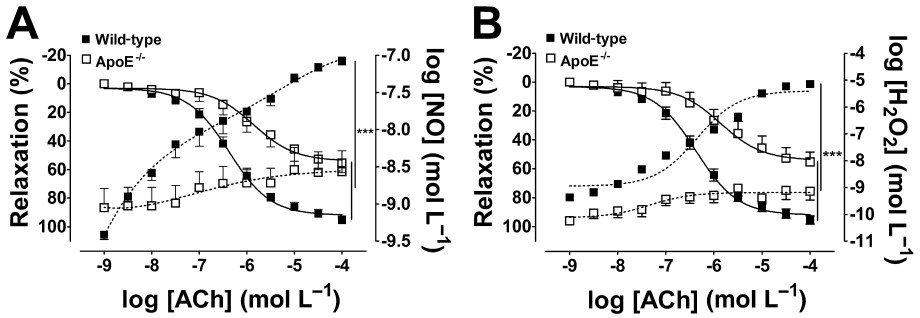


## Figure 1

Simultaneous measurements of vasodilatation (A,B), and NO (A) and $H_2O_2$ (B) production stimulated by ACh in the aortas of wild-type and ApoE$^{-/-}$ mice . Continuous lines represent vasodilatation (left axis); dotted lines: NO (A) and $H_2O_2$ (B) measurements (right axis). The data are shown as mean ± SEM of at least five experiments. ***$P < 0.001$.

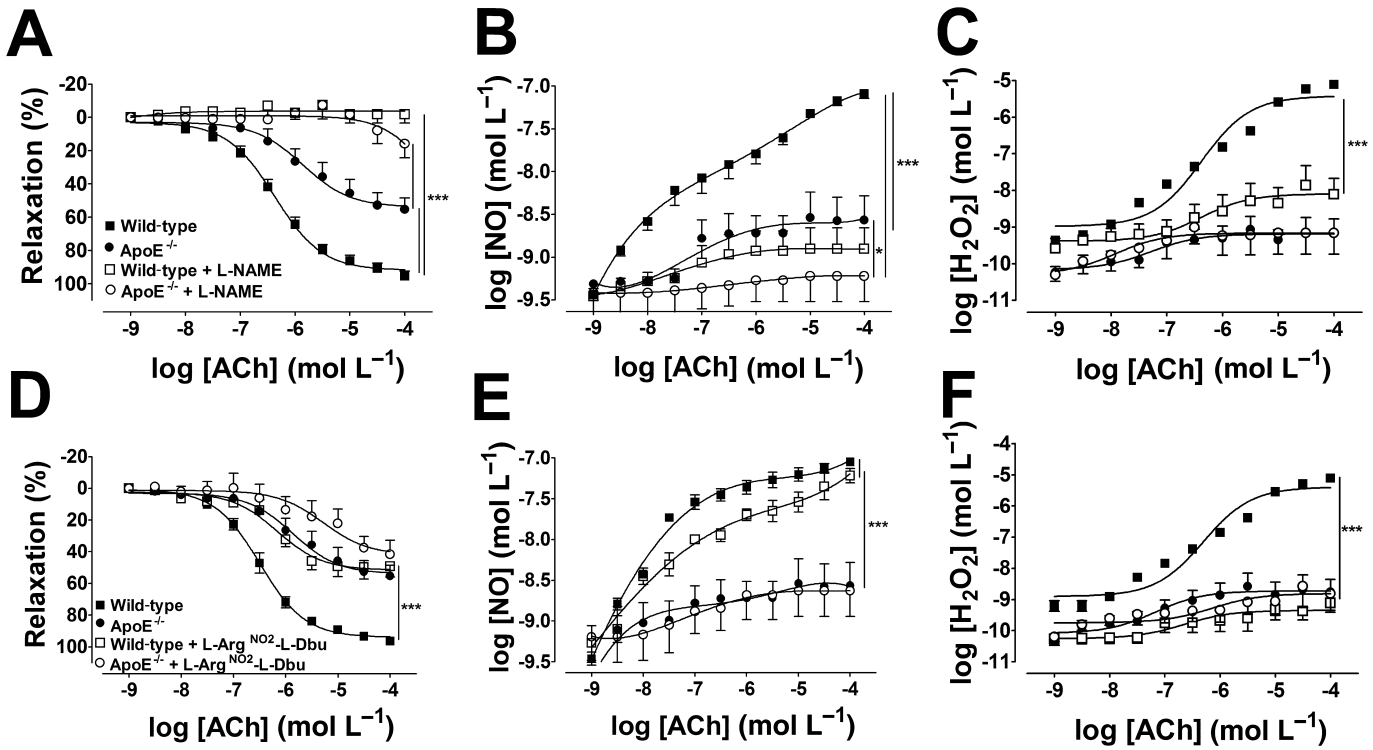


## Figure 2

(A–C) Effect of L-NAME (300 μmol·L$^{-1}$) on ACh-induced vasodilatation (A), NO (B) and $H_2O_2$ (C) production in the aortas of wild-type and ApoE$^{-/-}$ mice. (D–F) Selective pharmacological inhibition of nNOS with L-Arg$^{NO2}$-L-Dbu (1 μmol·L$^{-1}$) reduced vasodilatation in wild-type but not in ApoE$^{-/-}$ mice (D). In wild-type mice, L-Arg$^{NO2}$-L-Dbu produced a small reduction in NO production (E) and abolished $H_2O_2$ (F). NO (E) and $H_2O_2$ (F) were not modified by L-Arg$^{NO2}$-L-Dbu in ApoE$^{-/-}$ mice. The data represent mean ± SEM of at least five experiments. ***$P < 0.001$.

(Figure 3A,D). Confocal experiments to immunolocalize eNOS and nNOS showed that in the wild-type animals, both enzymes were present in the endothelial cells but were absent in the media layer (Figures 4A and 5A). In ApoE$^{-/-}$ arteries, eNOS (Figure 4C) and nNOS (Figure 5C) immunostaining were increased in the endothelium as compared with wild-type animals. Moreover, in ApoE$^{-/-}$ vessels, both enzymes were also shown to be present in the smooth muscle layer of the aorta (Figures 4A,B and 5A,B).

### *Determination of eNOS and nNOS phosphorylation by Western blot*

We analysed the phosphorylation state on serine (Ser) and threonine (Thr) sites of eNOS and nNOS by Western blot. In wild-type animals, ACh produced an increase in phosphorylation on Ser1177, the activation site of eNOS (Figure 3B); conversely, the phosphorylation state of the inactivation site of the enzyme on Thr495 was decreased (Figure 3C). In

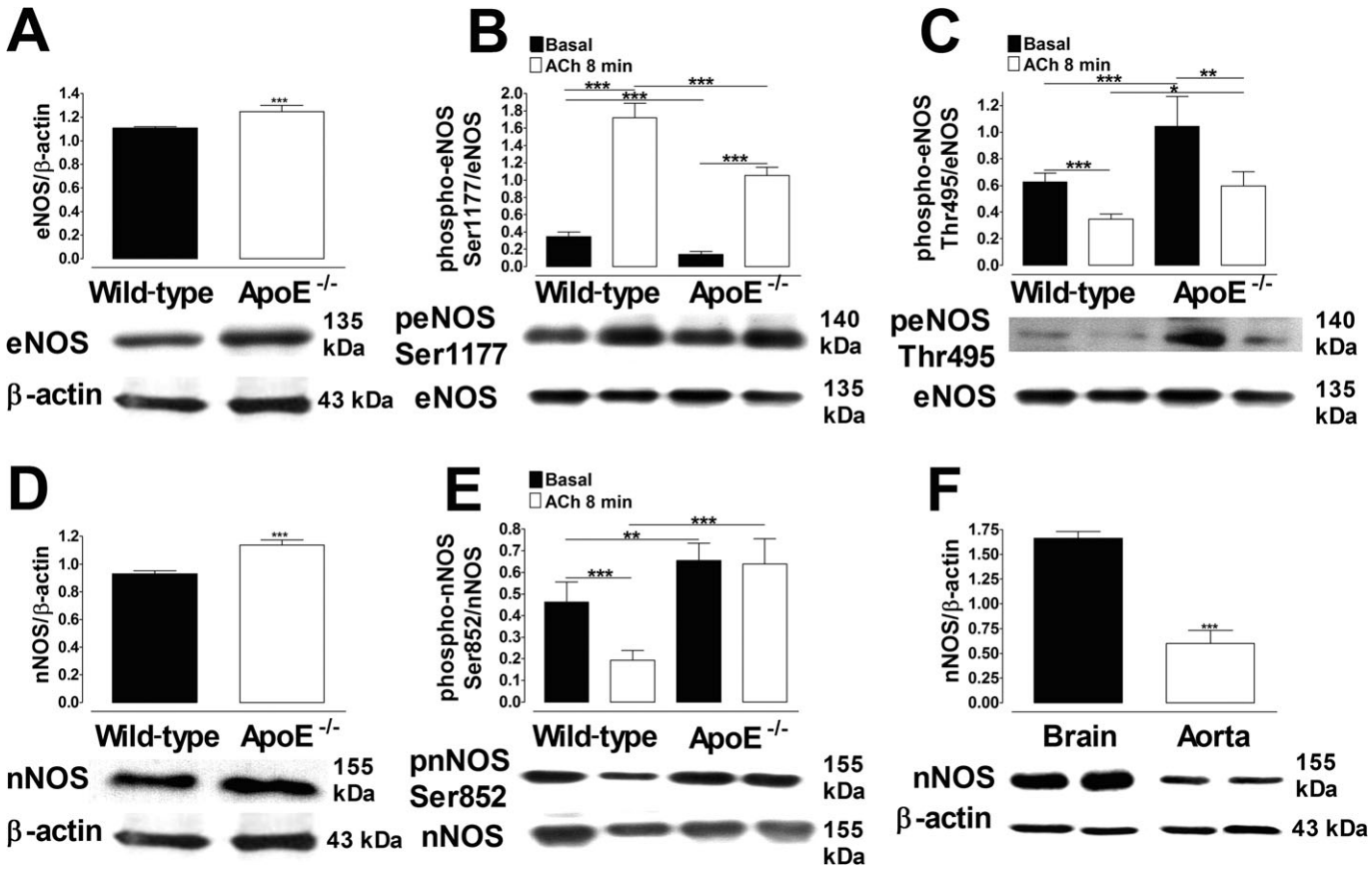


## Figure 3

eNOS (A) and nNOS (B) expression in aortas from wild-type and ApoE$^{-/-}$ mice. ACh-induced changes in the phosphorylation of eNOS-Ser1177 (B), eNOS-Thr495 (C) and nNOS-Ser852 (E). (F) Positive control for nNOS in brain. The vessels were stimulated with 100 μmol·L$^{-1}$ ACh. The histograms represent mean ± SEM of four experiments. ***$P < 0.001$; **$P < 0.01$. Images are representative blots from four separate experiments.

ApoE$^{-/-}$ mice, the increase in phosphorylation on eNOS-Ser1177 and dephosphorylation on eNOS-Thr495 induced by ACh was smaller compared with wild-type vessels (Figure 3B,C). Note that in basal conditions, ApoE$^{-/-}$ aortas also showed a less significant phosphorylation level on eNOS-Ser1177 and a higher level on eNOS-Thr495, compared with wild-type animals.

The inactivation site for nNOS on Ser852 showed higher phosphorylation levels on aortas from ApoE$^{-/-}$ mouse compared with control animals in the basal conditions. After stimulation with ACh, the phosphorylation level on the inactivation site of the enzyme was decreased in wild-type aorta but unchanged in ApoE$^{-/-}$ vessels (Figure 3E).

### *Vasodilator response, NO and $H_2O_2$ production in eNOS and nNOS knockdown animals*

The individual contribution of eNOS and nNOS to the vascular responses, and NO and $H_2O_2$ production in ApoE$^{-/-}$ mice, was evaluated by the use of *in vivo* AS-ODN knockdown of eNOS and nNOS expression. Wild-type eNOS-KD mice showed a reduced ACh-induced vasodilatation (Figure 6A) that was accompanied by a strong decrease in NO production (Figure 6B), without changes in $H_2O_2$ (Figure 6C). ACh-induced relaxation and NO production were attenuated in ApoE$^{-/-}$ eNOS-KD mice (Figure 6D,E). $H_2O_2$ production was already impaired in ApoE$^{-/-}$ aortas and was not modified in eNOS-KD animals (Figure 6F). Aortas from wild-type nNOS-KD mice showed reduced vascular responses to ACh (Figure 7A) in the same proportion as those seen with *in vitro* pharmacological inhibition of nNOS and with catalase, accompanied by a small reduction in NO production (Figure 7B). However, $H_2O_2$ synthesis was strongly decreased in these animals (Figure 7C). In aortas from ApoE$^{-/-}$ animals, nNOS knockdown did not change the relaxant response to ACh (Figure 7D), or the production of NO and $H_2O_2$ (Figure 7E,F). The ability of AS-ODN treatment to reduce eNOS and nNOS expression was confirmed by Western blot analysis as shown in Figure S4.

## Discussion and conclusions

The major finding of this work is that the function of endothelial nNOS in ApoE$^{-/-}$ mouse aorta is decreased, leading to a deficiency in $H_2O_2$ production and this contributes to the endothelial dysfunction in ApoE$^{-/-}$ mouse.

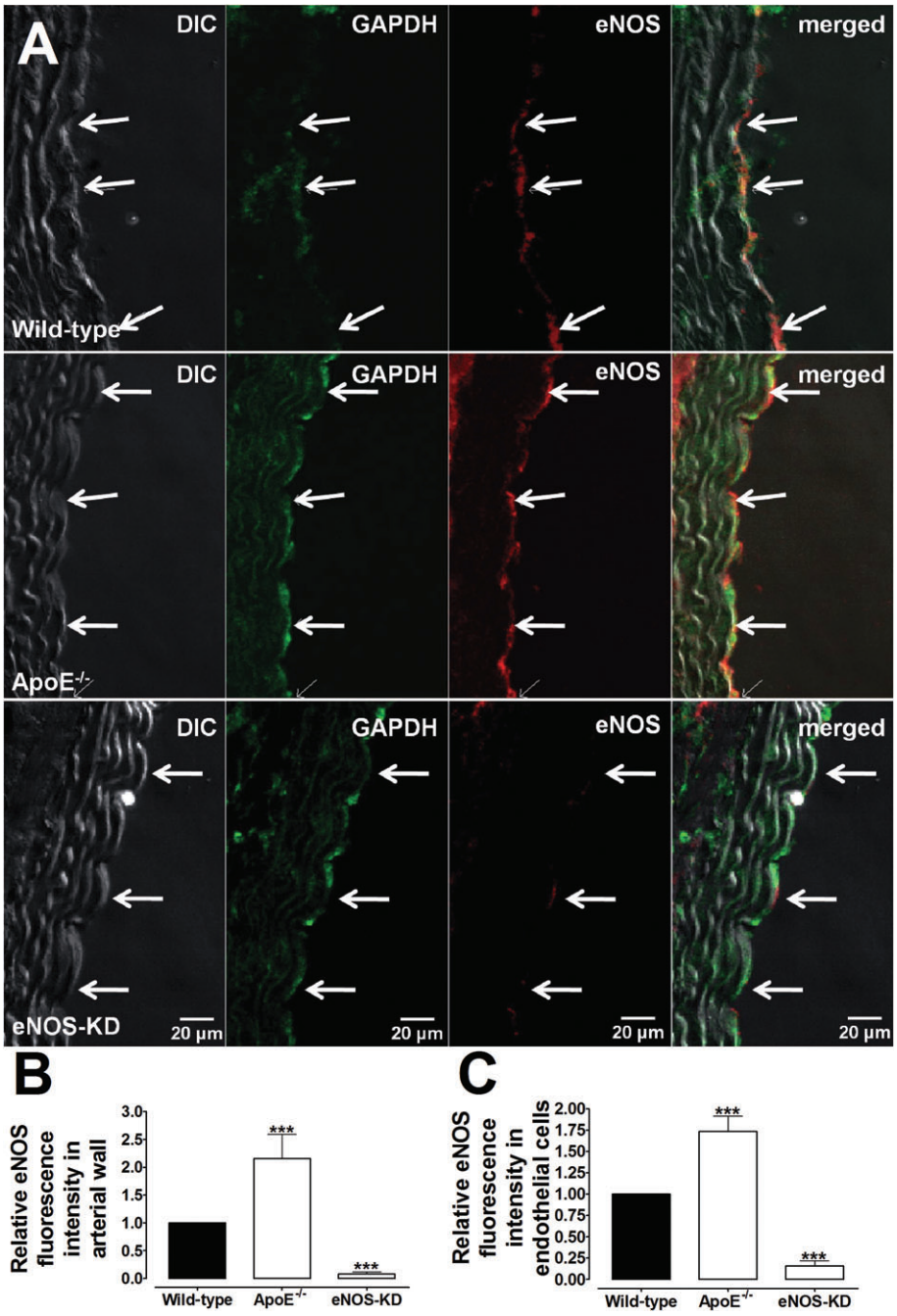


## Figure 4

Immunofluorescence detection of eNOS in aortic rings from wild-type (A, higher panel), ApoE$^{-/-}$ (A, middle panel) and eNOS-KD (A, lower panel) mice. Immunostaining for eNOS was present in endothelial cells (arrows) in wild-type and increased in ApoE$^{-/-}$ vessels. Note the strong decrease in eNOS immunostaining in eNOS KD (knockdown) animals. (B,C) The graphical representation of the relative eNOS fluorescence in the arterial wall (B) and in endothelial cells (C) from wild-type, ApoE$^{-/-}$ and eNOS-KD arteries. GAPDH was used for control loading purposes. Images are representative of five animals for each group. ***$P < 0.001$ compared with wild-type vessels.

It is well known that in the cardiovascular system, eNOS-derived NO plays an important role in the regulation of vascular tone (Garland *et al.*, 1995; Urakami-Harasawa *et al.*, 1997). However, there is increasing evidence attributing a physiologically relevant role for nNOS in the control of vascular homeostasis. The expression of nNOS in vascular smooth muscle and endothelial cells has been commonly associated with the control of brain blood flow (Wei *et al.*, 1999; Atochin *et al.*, 2003; Hagioka *et al.*, 2005; Kitaura *et al.*, 2007). In addition, in eNOS$^{-/-}$ mice, nNOS plays a major role in the control of the coronary circulation (Huang *et al.*, 2002; Talukder *et al.*, 2004; Chlopicki *et al.*, 2005). Recently, we

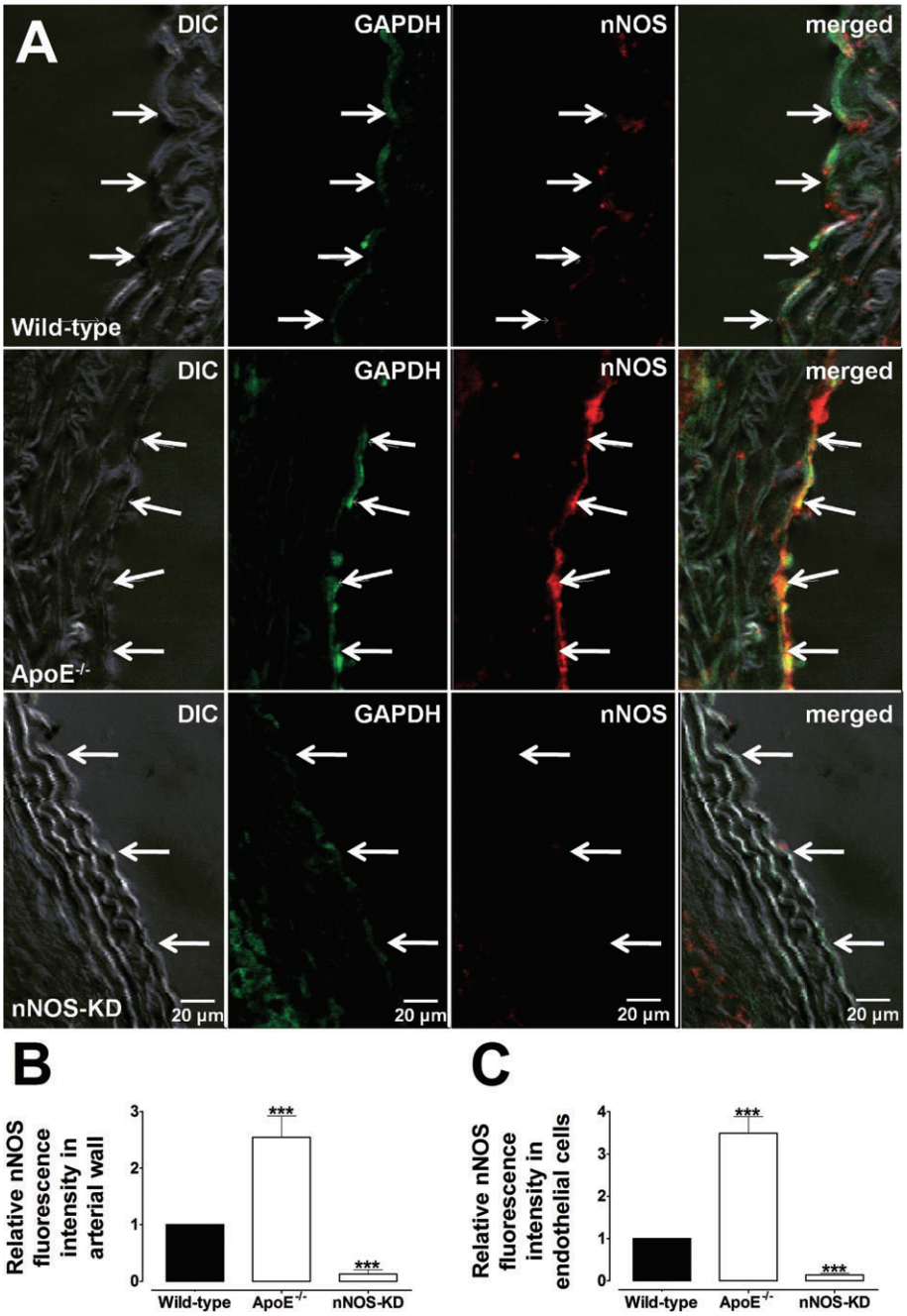


## Figure 5

Immunofluorescence detection of nNOS in aortic rings from wild-type (A, higher panel), ApoE$^{-/-}$ (A, middle panel) and nNOS-KD (A, lower panel) mice. Immunostaining for nNOS was increased in endothelial cells (arrows) from ApoE$^{-/-}$ compared with wild-type vessels. Staining in nNOS-KD (knockdown) animals was strongly diminished. (B,C) Graphical representation of the relative nNOS fluorescence in the arterial wall (B) and in endothelial cells (C) from wild-type, ApoE$^{-/-}$ and nNOS-KD arteries. GAPDH was used for control loading purposes. Images are representative of five animals for each group. ***$P < 0.001$ compared with wild-type vessels.

have shown that nNOS is constitutively expressed in the endothelium of mouse aorta and contributes to the endothelium-derived vasodilatation induced by ACh (Capettini *et al.*, 2008). These findings are consistent with the reduced vasodilatation found in the aorta from nNOS$^{-/-}$ mice (Nangle *et al.*, 2004). Interestingly, we have shown that besides NO, nNOS also produces $H_2O_2$ in physiological conditions. Using pharmacological inhibitors and antisense nNOS knockdown, and simultaneous measurement of NO, $H_2O_2$ and vascular function, we demonstrated that nNOS-derived $H_2O_2$ is a major endothelium-dependent relaxing factor in the mouse aorta and importantly contributes to endothelial-dependent vasodilatation in the mouse aorta (Rabelo *et al.*, 2003; Capettini *et al.*, 2008; 2010).

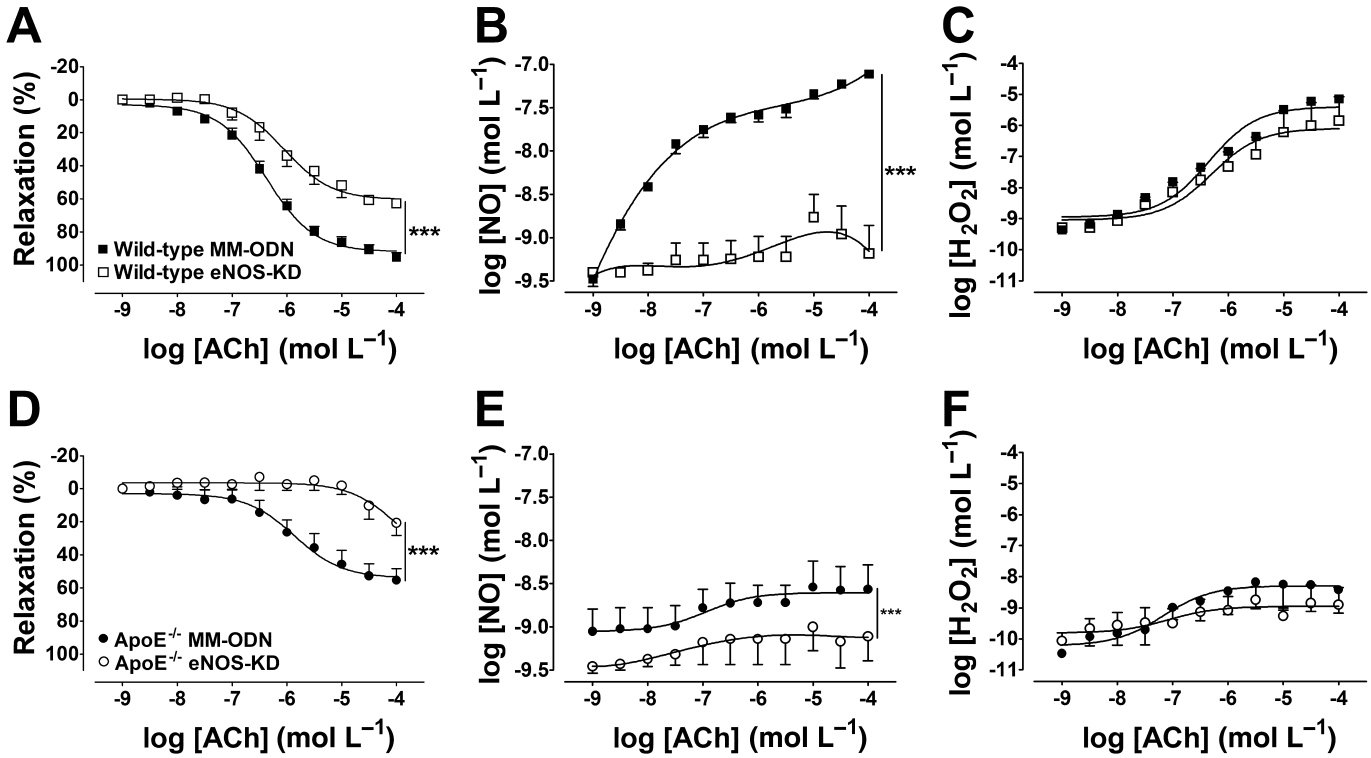


## Figure 6

Effect of *in vivo* antisense oligodeoxynucleotide eNOS knockdown (eNOS KD) on vasodilatation (A,D), NO (B,E) and $H_2O_2$ (C,F) production in aortas from wild-type (A–C) and ApoE$^{-/-}$ (D–F) mice. The data represent mean ± SEM of at least five experiments. ***$P < 0.001$.

It is well-established that endothelium-dependent vasodilatation is attenuated by hyperlipidaemia and atherosclerosis in animals (Busse and Fleming, 1996; Nangle *et al.*, 2003; Rabelo *et al.*, 2003) and human (Higashi *et al.*, 2009a; Toma *et al.*, 2009). Endothelial dysfunction in atherosclerosis has been commonly associated with a reduction in eNOS-derived NO bioavailability; the involvement of nNOS and $H_2O_2$ in endothelial dysfunction in atherosclerosis had not been clarified. In this work, we provide consistent evidence that an impairment in nNOS-derived $H_2O_2$ also contributes to endothelial dysfunction in the aorta from ApoE$^{-/-}$ mouse. In line with this proposal, selective pharmacological inhibition of nNOS reduced ACh-induced relaxation in control but not in ApoE$^{-/-}$ mouse. These results were further corroborated by specific antisense nNOS knockdown that showed similar results. These data point to a decreased function and/or expression of nNOS in ApoE$^{-/-}$ animals. However, the level of nNOS protein was increased in ApoE$^{-/-}$ mouse aortas, as assessed by Western blot analysis. Increased expression of nNOS in the media layer from ApoE$^{-/-}$ mice aortas has been reported previously (Schodel *et al.*, 2009).

Our confocal data showed the presence of nNOS immunostaining in the endothelial cell layer in control animals, consistent with previous reports using different assays (Loesch and Burnstock, 1998; Capettini *et al.*, 2008). Interestingly, we found that nNOS immunoreactivity was increased in the smooth muscle cell layer as well as in the endothelial cells from ApoE$^{-/-}$ mice aorta. Nonetheless, an important finding from the present work was the difference in the phosphorylation state of nNOS-Ser852, between the strains. In wild-type aortas ACh produced a decrease in phosphorylation of the inactivation site of the enzyme, while in ApoE$^{-/-}$ vessels nNOS-Ser852 remained unchanged by ACh stimulation. Together, these data indicate a decreased functioning of endothelial nNOS and suggest a role for this enzyme in the impaired vasorelaxation in the aorta from ApoE$^{-/-}$ mouse.

Oxidative stress has been implicated in impaired endothelium-dependent relaxations in atherosclerosis. An increased level of reactive oxygen species (ROS) in the vessel wall leads to modifications in calcium handling, expression of voltage-dependent L-type $Ca^{2+}$ channels, reduction in tetrahydrobiopterin availability and depletion of L-arginine in endothelial cells (Laursen *et al.*, 2001; Katusic and d'Uscio, 2004; Fransen *et al.*, 2008; Erdely *et al.*, 2010; Fu *et al.*, 2010). Therefore, we speculated that oxidative stress may well contribute to the reduced functionality of nNOS leading to impaired $H_2O_2$-induced relaxations.

The expression of eNOS was also reported to be increased in aortas from ApoE$^{-/-}$ mice in despite of the decreased NO production (Bouloumie *et al.*, 1997; Loesch and Burnstock, 1998; Laursen *et al.*, 2001; Kuhlencordt *et al.*, 2004). The decrease in NO production has been associated with changes in the phosphorylation state of the eNOS (Fernández-Hernando *et al.*, 2007; Wang *et al.*, 2010; Yamashiro *et al.*, 2010). Consistent with these data, we found an increased expression of eNOS in aortas from ApoE$^{-/-}$ mice and this was accompanied by a decreased vasodilator response, a

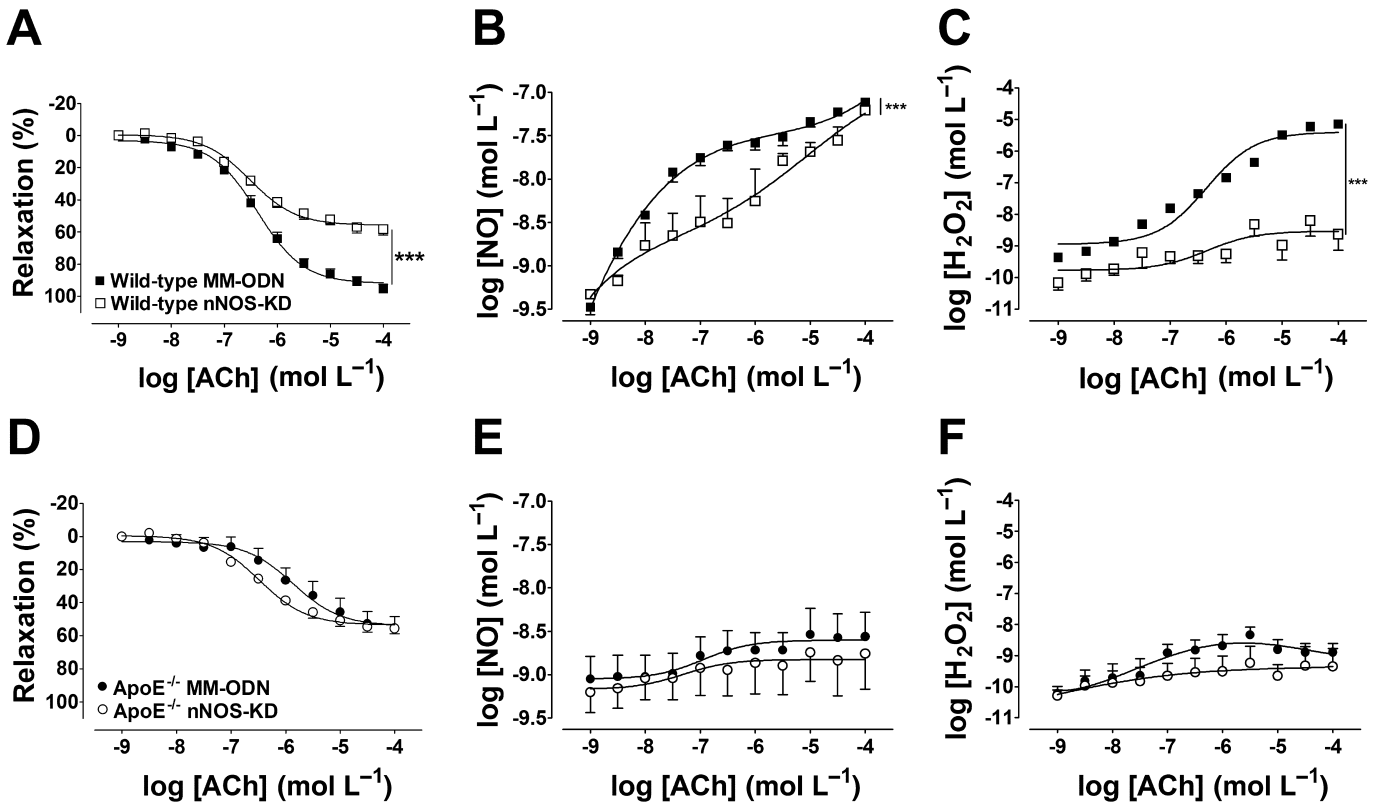


## Figure 7

Effect of *in vivo* antisense oligodeoxynucleotide nNOS knockdown (nNOS KD) on vasodilatation (A,D), NO (B,E) and $H_2O_2$ (C,F) production in aortas from wild-type (A–C) and ApoE$^{-/-}$ (D–F) mice. The data represent mean ± SEM of at least five experiments. ***$P < 0.001$.

diminution of eNOS function and a severe impairment in NO production.

In summary, our data show that vasodilatation in wild-type animals was decreased by half with catalase, nNOS knockdown or pharmacological nNOS inhibition. Endothelial dysfunction in ApoE$^{-/-}$ vessels was accompanied by abolishment of $H_2O_2$ production and vasorelaxation was not affected by catalase, nNOS knockdown or selective pharmacological nNOS inhibition. Conversely, eNOS knockdown abolished the vasorelaxation in ApoE$^{-/-}$ mice and reduced vasodilatation by half in wild-type animals. Vasodilatation in response to exogenous $H_2O_2$ was not different between strains. Together, these results show that (i) $H_2O_2$ production is suppressed in aortas from ApoE$^{-/-}$ animals and might contribute to the endothelial dysfunction in atherosclerosis; (ii) although severely impaired, NO accounts for the residual vasorelaxation in ApoE$^{-/-}$ mice.

In conclusion, our data show that endothelial nNOS activity is decreased in ApoE$^{-/-}$ mouse aorta. The reduced nNOS activity leads to an impairment in $H_2O_2$ production that contributes to the attenuated endothelium-dependent vasodilator response. These results indicate a new mechanism for endothelial dysfunction showing a critical role for nNOS-derived $H_2O_2$ in the impaired vasodilator response in atherosclerosis. nNOS may represent a novel target to elaborate the therapeutic strategy for vascular atherosclerosis.

## Acknowledgements

This study was supported by FAPEMIG (Fundação de Apoio a Pesquisa do Estado de Minas Gerais), CNPq/Brazil (Conselho Nacional de Desenvolvimento Científico e Tecnológico) and CAPES (Coordenação de Aperfeiçoamento de Pessoal de Nível Superior).

## Conflict of interest

The authors state no conflict of interest.

## References

Alderton WK, Cooper CE, Knowles RG (2001). Nitric oxide synthases: structure, function and inhibition. Biochem J 357: 593–615.

Atochin DN, Demchenko IT, Astern J, Boso AE, Piantadosi CA, Huang PL (2003). Contributions of endothelial and neuronal nitric oxide synthases to cerebrovascular responses to hyperoxia. J Cereb Blood Flow Metab 23: 1219–1226.

Bachetti T, Comini L, Curello S, Bastianon D, Palmieri M, Bresciani G *et al.* (2004). Co-expression and modulation of neuronal and endothelial nitric oxide synthase in human endothelial cells. J Mol Cell Cardiol 37: 939–945.

Boulanger CM, Heymes C, Benessiano J, Geske RS, Levy BI, Vanhoutte PM (1998). Neuronal nitric oxide synthase is expressed in rat vascular smooth muscle cells: activation by angiotensin II in hypertension. Circ Res 83: 1271–1278.

Bouloumie A, Bauersachs J, Linz W, Scholkens BA, Wiemer G, Fleming I *et al.* (1997). Endothelial dysfunction coincides with an enhanced nitric oxide synthase expression and superoxide anion production. Hypertension 30: 934–941.

Busse R, Fleming I (1996). Endothelial dysfunction in atherosclerosis. J Vasc Res 33: 181–194.

Cai H, Harrison DG (2000). Endothelial dysfunction in cardiovascular diseases: the role of oxidant stress. Circ Res 87: 840–844.

Capettini LS, Cortes SF, Gomes MA, Silva GA, Pesquero JL, Lopes MJ *et al.* (2008). Neuronal nitric oxide synthase-derived hydrogen peroxide is a major endothelium-dependent relaxing factor. Am J Physiol Heart Circ Physiol 295: H2503–H2511.

Capettini LS, Cortes SF, Lemos VS (2010). Relative contribution of eNOS and nNOS to endothelium-dependent vasodilation in the mouse aorta. Eur J Pharmacol 643: 260–266.

Chlopicki S, Kozlovski VI, Lorkowska B, Drelicharz L, Gebska A (2005). Compensation of endothelium-dependent responses in coronary circulation of eNOS-deficient mice. J Cardiovasc Pharmacol 46: 115–123.

Deckert V, Lizard G, Duverger N, Athias A, Palleau V, Emmanuel F *et al.* (1999). Impairment of endothelium-dependent arterial relaxation by high-fat feeding in ApoE-deficient mice: toward normalization by human ApoA-I expression. Circulation 100: 1230–1235.

Erdely A, Kepka-Lenhart D, Salmen-Muniz R, Chapman R, Hulderman T, Kashon M *et al.* (2010). Arginase activities and global arginine bioavailability in wild-type and ApoE-deficient mice: responses to high fat and high cholesterol diets. PLoS ONE 5: e15253.

Fernández-Hernando C, Ackah E, Yu J, Suárez Y, Murata T, Iwakiri Y *et al.* (2007). Loss of Akt1 leads to severe atherosclerosis and occlusive coronary artery disease. Cell Metab 6: 446–457.

Fleming I (2003). Brain in the brawn: the neuronal nitric oxide synthase as a regulator of myogenic tone. Circ Res 93: 586–588.

Fransen P, Van Assche T, Guns PJ, Van Hove CE, De Keuleaner GW, Herman AG *et al.* (2008). Endothelial function in aorta segments of apolipoprotein E-deficient mice before development of atherosclerotic lesions. Pflugers Arch 455: 811–815.

Freedman JE, Sauter R, Battinelli EM, Ault K, Knowles C, Huang PL *et al.* (1999). Deficient platelet-derived nitric oxide and enhanced hemostasis in mice lacking the NOSIII gene. Circ Res 84: 1416–1421.

Fu C, He J, Li C, Shyy JYJ, Zhu Y (2010). Cholesterol increases adhesion of monocytes to endothelium by moving adhesion molecules out of caveolae. Biochim Biophys Acta 1801: 702–710.

Garland CJ, Plane F, Kemp BK, Cocks TM (1995). Endothelium-dependent hyperpolarization: a role in the control of vascular tone. Trends Pharmacol Sci 16: 23–30.

Hagioka S, Takeda Y, Zhang S, Sato T, Morita K (2005). Effects of 7-nitroindazole and N-nitro-L-arginine methyl ester on changes in cerebral blood flow and nitric oxide production preceding development of hyperbaric oxygen-induced seizures in rats. Neurosci Lett 382: 206–210.

Higashi Y, Maysuoka H, Umei H, Sugano R, Fujii Y, Soga J *et al.* (2009a). Endothelial function in subjects with isolated low HDL cholesterol: role of nitric oxide and circulating progenitor cells. Am J Physiol Endocrinol Metab 298: e202–e209.

Higashi Y, Noma K, Yoshizumi M, Kihara Y (2009b). Endothelial function and oxidative stress in cardiovascular diseases. Circ J 73: 411–418.

Huang A, Sun D, Shesely EG, Levee EM, Koller A, Kaley G (2002). Neuronal NOS-dependent dilation to flow in coronary arteries of male eNOS-KO mice. Am J Physiol Heart Circ Physiol 282: H429–H436.

Huang H, Martasek P, Roman LJ, Masters BSS, Silverman RB (1999). Nω-Nitroarginine-containing dipeptide amides. Potent and highly selective inhibitors of neuronal nitric oxide synthase. J Med Chem 42: 3147–3153.

Iida Y, Katusic ZS (2000). Mechanisms of cerebral arterial relaxations to hydrogen peroxide. Stroke 31: 2224–2230.

Katusic ZS, d'Uscio LV (2004). Tetrahydrobiopterin: mediator of endothelial protection. Arterioscler Thromb Vasc Biol 24: F552–F558.

Kitaura H, Uozumi N, Tohmi M, Yamazaki M, Sakimura K, Kudoh M *et al.* (2007). Roles of nitric oxide as a vasodilator in neurovascular coupling of mouse somatosensory cortex. Neurosci Res 59: 160–171.

Kubes P, Suzuki M, Granger DN (1991). Nitric oxide: an endogenous modulator of leukocyte adhesion. Proc Natl Acad Sci U S A 88: 4651–4655.

Kuhlencordt PJ, Rosel E, Gerszten RE, Morales-Ruiz M, Dombkowski D, Atkinson WJ *et al.* (2004). Role of endothelial nitric oxide synthase in endothelial activation: insights from eNOS knockout endothelial cells. Am J Physiol Cell Physiol 286: C1195–C1202.

Kuhlencordt PJ, Hotten S, Schodel J, Rutzel S, Hu K, Widder J *et al.* (2006). Atheroprotective effects of neuronal nitric oxide synthase in apolipoprotein-e knockout mice. Arterioscler Thromb Vasc Biol 26: 1539–1544.

Kurihara N, Alfie ME, Sigmon DH, Rhaleb NE, Shesely EG, Carretero OA (1998). Role of nNOS in blood pressure regulation in eNOS null mutant mice. Hypertension 32: 856–861.

Laursen JB, Somers M, Kurz S, McCann L, Warnholtz A, Freeman BA *et al.* (2001). Endothelial regulation of vasomotion in apoE-deficient mice: implications for interactions between peroxynitrite and tetrahydrobiopterin. Circulation 103: 1282–1288.

Leopold JA, Loscalzo J (2009). Oxidative risk for atherothrombotic cardiovascular disease. Free Radic Biol Med 47: 1673–1706.

Loesch A, Burnstock G (1998). Perivascular nerve fibres and endothelial cells of the rat basilar artery: immuno-gold labelling of antigenic sites for type I and type III nitric oxide synthase. J Neurocytol 27: 197–204.

Luscher TF, Barton M (1997). Biology of the endothelium. Clin Cardiol 20: II3–II10.

Matoba T, Shimokawa H, Nakashima M, Hirakawa Y, Mukai Y, Hirano K *et al.* (2000). Hydrogen peroxide is an endothelium-derived hyperpolarizing factor in mice. J Clin Invest 106: 1521–1530.

Matoba T, Shimokawa H, Kubota H, Morikawa K, Fujiki T, Kunihiro I *et al.* (2002). Hydrogen peroxide is an endothelium-derived hyperpolarizing factor in human mesenteric arteries. Biochem Biophys Res Commun 290: 909–913.

Miura H, Bosnjak JJ, Ning G, Saito T, Miura M, Gutterman DD (2003). Role for hydrogen peroxide in flow-induced dilation of human coronary arterioles. Circ Res 92: e31–e40.

Morishita T, Tsutsui M, Shimokawa H, Horiuchi M, Tanimoto A, Suda O *et al*. (2002). Vasculoprotective roles of neuronal nitric oxide synthase. FASEB J 16: 1994–1996.

Nangle MR, Cotter MA, Cameron NE (2003). Effects of rosuvastatin on nitric oxide-dependent function in aorta and corpus cavernosum of diabetic mice: relationship to cholesterol biosynthesis pathway inhibition and lipid lowering. Diabetes 52: 2396–2402.

Nangle MR, Cotter MA, Cameron NE (2004). An *in vitro* investigation of aorta and corpus cavernosum from eNOS and nNOS gene-deficient mice. Eur J Physiol 448: 139–145.

Rabelo LA, Cortes SF, Alvarez-Leite JI, Lemos VS (2003). Endothelium dysfunction in LDL receptor knockout mice: a role for $H_2O_2$. Br J Pharmacol 138: 1215–1220.

Rosenblum WI, Murata S (1996). Antisense evidence for two functionally active forms of nitric oxide synthase in brain microvascular endothelium. Biochem Biophys Res Commun 224: 535–543.

Ross R (1999). Atherosclerosis is an inflammatory disease. Am Heart J 138: S419–S420.

Schodel J, Padmapriya P, Marx A, Huang PL, Ertl G, Kuhlencordt PJ (2009). Expression of neuronal nitric oxide synthase splice variants in atherosclerotic plaques of apoE knockout mice. Atherosclerosis 206: 383–389.

Shimokawa H (1999). Primary endothelial dysfunction: atherosclerosis. J Mol Cell Cardiol 31: 23–37.

Sima AV, Stancu CS, Simionescu M (2009). Vascular endothelium in atherosclerosis. Cell Tissue Res 335: 191–203.

Sobey CG, Heistad DD, Faraci FM (1997). Mechanisms of bradykinin-induced cerebral vasodilatation in rats. Evidence that reactive oxygen species activate K+ channels. Stroke 28: 2290–2295.

Talukder MA, Fujiki T, Morikawa K, Motoishi M, Kubota H, Morishita T *et al*. (2004). Up-regulated neuronal nitric oxide synthase compensates coronary flow response to bradykinin in endothelial nitric oxide synthase-deficient mice. J Cardiovasc Pharmacol 44: 437–445.

Toda N, Okamura T (2003). The pharmacology of nitric oxide in the peripheral nervous system of blood vessels. Pharmacol Rev 55: 271–324.

Toma L, Stancu CS, Botez GM, Sima AV, Simionescu M (2009). Irreversibly glycated LDL induce oxidative and inflammatory state in human endothelial cells; added effect of high glucose. Biochem Biophys Res Commun 390: 877–882.

Tsutsui M (2004). Neuronal nitric oxide synthase as a novel anti-atherogenic factor. J Atheroscler Thromb 11: 41–48.

Urakami-Harasawa L, Shimokawa H, Nakashima M, Egashira K, Takeshita A (1997). Importance of endothelium-derived hyperpolarizing factor in human arteries. J Clin Invest 100: 2793–2799.

Vanhoutte PM (1986). The endothelium and arterial reactivity. J Mal Vasc 11: 213–221.

Wang F, Okamoto Y, Inoki I, Yoshioka K, Du W, Qi X *et al.* (2010). Sphingosine-1-phosphate receptor-2 deficiency leads to inhibition of macrophage proinflammatory activities and atherosclerosis in apoE-deficient mice. J Clin Invest 120: 3979–3995.

Wei G, Dawson VL, Zweier JL (1999). Role of neuronal and endothelial nitric oxide synthase in nitric oxide generation in the brain following cerebral ischemia. Biochim Biophys Acta 1455: 23–34.

Wilcox JN, Subramanian RR, Sundell CL, Tracey WR, Pollock JS, Harrison DG *et al*. (1997). Expression of multiple isoforms of nitric oxide synthase in normal and atherosclerotic vessels. Arterioscler Thromb Vasc Biol 17: 2479–2488.

Yada T, Shimokawa H, Hiramatsu O, Kajita T, Shigeto F, Goto M *et al*. (2003). Hydrogen peroxide, an endogenous endothelium-derived hyperpolarizing factor, plays an important role in coronary autoregulation *in vivo*. Circulation 107: 1040–1045.

Yamashiro K, Milsom AB, Duchene J, Panayiotou C, Urabe T, Hattori N *et al*. (2010). Alterations in nitric oxide and endothelin-1 bioactivity underlie cerebrovascular dysfunction in ApoE-deficient mice. J Cereb Blood Flow Metab 30: 1494–1503.

## Supporting information

Additional Supporting Information may be found in the online version of this article:

**Figure S1** Morphological analyses in the structure of the aortic arch (A) and thoracic aorta (B) from wild-type and $ApoE^{-/-}$ mice. Representative H&E-stained sections from 5 experiments. Scale bar: 10 μm.
**Figure S2** Effect of catalase (2400 $U \cdot mL^{-1}$) on vasodilation induced by ACh on wild-type and $ApoE^{-/-}$ mice aortas. The data represent mean ± SEM of five experiments. ***$P < 0.001$.
**Figure S3** Vasodilator effect of exogenous $H_2O_2$ in aortas from wild type and $ApoE^{-/-}$ mice. The experiments were performed in the presence of 50 $mmol \cdot L^{-1}$ aminotriazole (Sigma) to inhibit endogenous peroxidises. The data represent mean ± SEM of five experiments.
**Figure S4** Western-blot analysis of the effect of *in vivo* antisense eNOS (eNOS-KD; A) and nNOS (n-NOS-KD; B) knockdown in wild-type and $ApoE^{-/-}$ mice aorta. (C) Control experiments for nNOS in eNOS-KD animals and (D) controls Western blot for eNOS in nNOS-KD aortas. Images are representative of four experiments. Bar graphs represent mean ± SEM of four experiments. ***$P < 0.001$.

Please note: Wiley-Blackwell are not responsible for the content or functionality of any supporting materials supplied by the authors. Any queries (other than missing material) should be directed to the corresponding author for the article.